

Component 1: Urate Oxidase

Shane Kalani Abbley

Abstract:

The ultimate goal of this series of experiments is to determine the effect that the F182Y mutation has on the urate oxidase activity. In the first component of this analysis, we designed an experiment to produce a mutated enzyme variant from *Bacillus subtilis*. The F182Y mutation introduced a one amino acid mutation that transformed phenylalanine to tyrosine at position 182 in the amino acid sequence of urate oxidase. We created the mutation using specifically designed primers and a PCR based replication of our plasmids. We then transformed these mutant plasmids into host competent cells. We then ran an electrophoresis gel to determine the identity of our plasmid. Unlike similar experiments where the gel could be used to determine the success of the mutation, our mutation did not confer with a plasmid digest that would differentiate between the wild type and mutant variants. For this reason, we relied on an outsourced capillary electrophoresis to confirm the identity of our mutation. We will continue with characterization of the expressed protein in the next component of this experiment.

Primary Experimental Objective:

In component one of this experiment the primary objective is to create a mutant urate oxidase gene, such that when expressed amino acid 182 is transformed from a phenylalanine residue to a tyrosine residue. We will utilize biochemistry techniques including: PCR, site directed mutagenesis, competent cell transformation, plasmid purification, gel electrophoresis, and finish by sequencing our mutated plasmid.

Introduction:

Urate oxidase is a homotetrameric protein that catalyzes the formation of 5-hydroxyisourate and hydrogen peroxide by oxidizing uric acid with molecular oxygen¹. This enzyme has two nonsense mutations in humans and other higher primates, but is active in many other animals, plants, fungi, and bacteria². *Bacillus subtilis* in particular has a frequently studied variant of this

enzyme. This urate oxidase isoform is cheap to obtain, easy to isolate, and is fairly well characterized already. This enzyme is relevant to scientific study because of its previous successful treatment of gout and tumor lysis syndrome³. Gout is characterized by a build up of crystals of uric acid, specifically within joints⁴. Tumor lysis syndrome also correlates to high uric acid concentrations and typically occurs after chemotherapy treatments⁴. There are several treatments for both of these disorders, but the more effective treatments are extremely expensive⁵. For these reasons the research and development of alternative treatments strategies is appealing to public and private investing.

Our residue of interest is a phenylalanine at position 182 in the wild type protein. We performed a multiple sequence analysis at the beginning of this experiment to determine the frequency of this residue amongst many different species. We discovered that this is a conserved aromatic amino acid residue. It is believed to stabilize phenylalanine 179, which in turn stacks against the heteroaromatic ring in urate¹.

The primers were designed such that the nucleotide substitution occurs near the middle of the primer and that the codon would express tyrosine rather than phenylalanine. This phenylalanine residue is of interest to us so that we may acquire a better understanding of how it interacts with the active site residues and thus how it affects the rate of catalysis. It is likely that a transformation from phenylalanine to tyrosine would result in a change in activity because of the addition of the hydroxyl group. This substitution alters the pi stacking energy, ΔE , where the $\Delta E_{\text{Phenylalanine}} > \Delta E_{\text{Tyrosine}}$ ⁵. Considering this, we hypothesize a decrease in stabilization energy after the mutation and potentially less favorable energetics between the active site and urate oxidase, resulting in loss of enzyme activity. That being said, the change is minor enough that the activity of the mutant should be comparable to the wild type.

A pWhitescript plasmid should also provide a reference point for our mutant during gel electrophoresis. This plasmid was chosen because it is easy to visualize. PWhitescript plasmid expresses a β -galactosidase gene in the presence of our primer⁴. β -galactosidase catalyzes the hydrolysis of X-gal into 5-bromo-4-chloro-3-hydroxy-indole. Two of these intermediates react irreversibly to form a deep blue visual marker. All pWhitescript *E. coli* cells that have

transformed the successful PCR reaction product will express this protein and color. Those who do not will appear white rather than blue. Following the site directed mutagenesis, the DpnI is added to separate out native DNA from our plasmid DNA. This occurs because DpnI targets methylated DNA, unlike most restriction endonucleases, which target nonnative unmethylated DNA.¹ This also relates to the choice of our competent cells. Our competent cells are nuclease deficient allowing us to use DpnI for this separation. Our host XL1-Blue cells also do not express T7 RNA polymerase, which is required for the expression of our urate oxidase gene in the pET-14b plasmid¹. Our β -lactamase gene promoter is recognized by the host cell polymerases and thus our ampicillin will be expressed. This is why we put ampicillin on our plates, to select for cells that have uptaken the plasmid. The plasmid is only able to enter the host cell after heating and cooling in calcium ion mediated pore formation. The calcium interacts with the negatively charged DNA and is attracted to the negatively charged surface of the bacteria¹. The high concentration of DNA near the surface of the cell can now enter the more permeable membrane after the heat shock and the influx of water following the chloride ions¹.

During the purification of our plasmids we capture our plasmid DNA in a positively charged silica matrix so that we can remove the undesired proteins and chromosomal DNA. SDS to disrupt the cell membrane and to denature undesired proteins. The sodium hydroxide denatures DNA and the RNase degrades RNA in the solution. Upon addition of the chaotropic salts, the DNA reanneals and the proteins continue to break down. Our plasmid DNA will reform appropriately, but the chromosomal DNA reforms incorrectly into long and easy to separate strands. After removing the contaminants the plasmid DNA can be eluted using a low ionic strength solution. We measure the spectrum of our sample because the bases of the nucleotides have specific absorbance values as do the aromatic amino acid residues. Specifically, A_{260} represents the maximum absorbance wavelength of nucleobases and A_{280} represents the maximum absorbance wavelength of aromatic amino acids¹. At A_{320} the absorbance of DNA should be practically zero and should not be more than 10% of the A_{260} value¹. Any significant error here would indicate that a contaminant is present. The ratio of A_{260}/A_{280} should be greater than 1.7 to be considered a successful purification of plasmid DNA¹.

Our final gel will reaffirm the presence of our plasmid, but it will not inform us of the presence of our mutation. Our mutation was such that there is no available restriction endonuclease that would allow us to see base pair values indicating a successful mutation. We will still evaluate the bands we obtain after a digest with the restriction endonuclease PstI.

Methods:

Site Directed Mutagenesis:

We started this experiment by designing and ordering the following primers, where the mutation is highlighted red:

5' - GGC AAC TCC TTC GTC GGC T **AC** ATC CGG GAC GAA TAT ACG - 3'

3' - CCG TTG AGG AAG CAG CCG A **TG** TAG GCC CTG CTT ATA TGC - 5'

N - GLY ASN SER PHE VAL GLY **TYR** ILE ARG ASP GLU TYR THR.

Using control primers, the appropriate buffer, dDTP's, and the control plasmid we created a control group for this experiment. We then added the PfuUltra DNA polymerase to the control group. Next, we ran this in the thermocycler for 16 cycles at 95 °C, 55 °C, 68 °C for 50 s, 60 s, and 6-8 minutes, respectively. We repeated this procedure with our mutant, except we used our mutant primers and the pET-14 b plasmid. Also, the annealing temperature for the mutation was decreased to 55 °C. After completion of PCR cycles we added 1.0 µL DpnI and incubated the mixture for 1 hour at 37 °C. We performed a gel electrophoresis test on these plasmid products on a 0.9% agarose TAE gel run at 80 V and stained with SYBR Safe dye.

Bacterial Cell Transformation #1:

50 µL of XL1-Blue strain (*E. coli*) competent cells were dethawed and combined with 1.0 µL of control and mutant DpNI-treated DNA. We incubated on ice for 25 minutes. The cells were then heat shocked at 42 °C for 45 seconds. Immediately after the cells were rested on ice for 2 minutes. 0.5 mL of warm SOC was added to both tubes. Incubation for 45 minutes at 37 °C while shaking ensued (250 rpm). We prepared two agar plates. The plate for the pWhitescript control contained ampicillin, IPTG, and X-gal, while the mutant plate only contained ampicillin.

We centrifuged both for 1 minute at 7,000 rpm, then removed all but 100.0 μL of supernatant. We pipetted 100.0 μL of resuspended transformation reactions onto their respective plates. Lastly we let the plates incubate for 20 hours at 37 $^{\circ}\text{C}$.

Bacterial Multiplication and Plasmid Purification:

Two sterile culture tubes were prepared with 4.0 mL of LB and 100 $\mu\text{g/mL}$ ampicillin. One colony of bacteria from each plate was added to separate tubes and inoculated for 12 hours. Then we incubated the cells for 12 hours while shaking at 250 rpm at 37 $^{\circ}\text{C}$. Centrifugation of 1.8 mL of cell suspension on maximum speed for 1 minute precipitated a cell pellet. We discarded the supernatant and added 100.0 μL Tris-EDTA buffer containing 50.0 $\mu\text{g/mL}$ of RNase A. After mixing, we added 100.0 μL of 0.2 M NaOH and 1% SDS (w/v) solution. We then added 125.0 μL of guanidinium hydrochloride in acetic acid and centrifuged this solution at maximum speed for 5 minutes. We transferred the supernatant to a microspin cup, containing the fiber matrix, and spun in a microcentrifuge at maximum speed for 30 seconds. After discarding the liquid, we separated out the endonucleases using 750.0 μL of more guanidinium hydrochloride in an isopropanol-water mixture, and centrifuged at maximum speed for 30 seconds 2 times. This centrifugation was repeated after adding 750 μL of a wash buffer containing 5.0 mM Tris HCl, 50.0 mM NaCl, and 1.25 mM EDTA to a 50:50 ethanol in water mixture. The sample was incubated for 5 minutes in 40.0 μL of 10.0 mM Tris and HCl (pH 8.5). Lastly, we centrifuged the sample one last time at maximum speed for 30 seconds. We then measured a spectrophotometric reading of our sample diluted by a factor of 10 in water to determine the concentration and purity of our plasmid DNA. We collected measurements under the parameters: 240 nm to 340 nm and 0 absorbance to 0.5 absorbance.

Restriction Digest and Agarose Gel Electrophoresis:

We first prepared our agarose gel using 250.0 mL of 1X TAE and 1.3% agarose. We then placed 2.5 μL of the 1 kilobase ladder in the two outer lanes. The two samples we loaded are the purified control plasmid and the purified mutant plasmid, which were prepared using 4.0 μL NEBuffer 3.1 and the PstI restriction enzyme. This was mixed with an equal volume of plasmid sample and 1.5 μL of 6X loading dye. We covered the gel in the mold with about 1.0 mm of buffer and pipetted our samples. We set the apparatus to 100 V and let it run for about 45

minutes or until the yellow indicator was near the edge of the gel. We stained the gel in the dark for 25 minutes in a solution containing 5.0 μL of SYBR Safe dye in 50.0 mL of NEBuffer 3.1. Lastly, the gel was imaged. The image of the gel in the results below was labeled and edited for clarity.

Plasmid DNA Sequencing:

We sent an aliquot of about 500 ng of our plasmid DNA in 10.0 μL of water to UC Berkeley's sequencing facilities. They returned our sequence digitally and it is partially presented below. PstI was chosen because it was expected to cut the plasmid two times creating two expected bands.

Experimental Results:

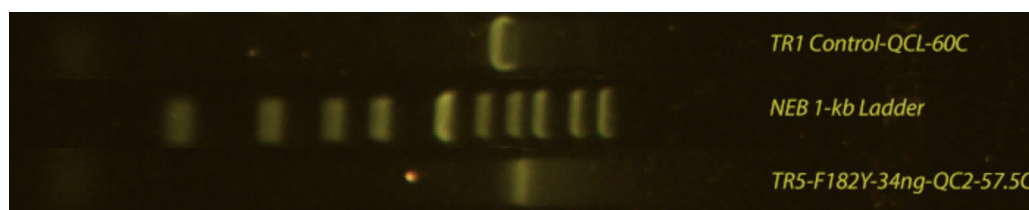


Figure 1: This figure shows our initial agarose gel following site directed mutagenesis. On the top is our control group urate oxidase gene (~4.5 kb) and on the bottom is our mutated urate oxidase gene (~5.5 kb).

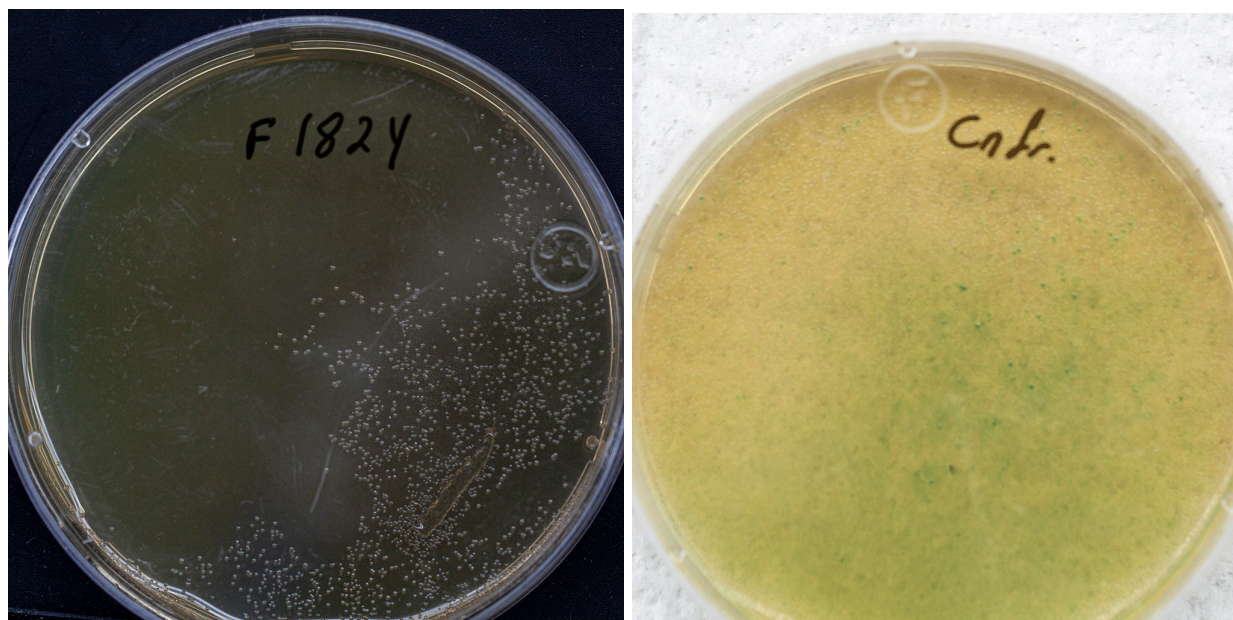


Figure 2 Left: F182Y mutant colonies of transformed XL1 bacteria on ampicillin and agar plate.

Figure 2 Right: Control colonies of transformed XL1 bacteria on an agar plate containing ampicillin, IPTG, and X-Gal.

Absorbance of Purified Mutant Plasmid

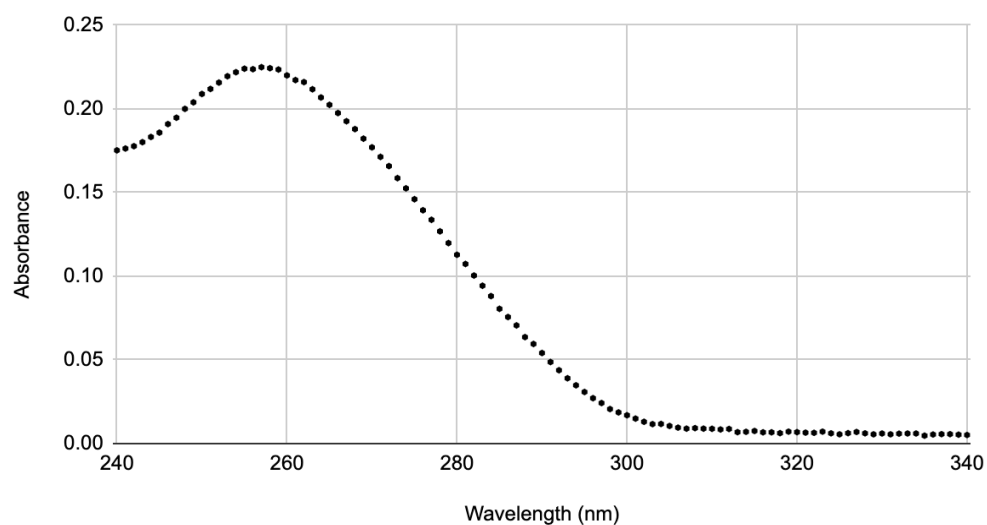


Figure 3: This graph shows the absorbance of the mutant F182Y purified plasmid as a function of wavelength.

Ratio of Absorbances 260/280	Concentration in Dilute Cuvette	Concentration in Purified Plasmid Solution
1.95035461	10.6 ng/mL	106 ng/mL

Figure 4: These values were obtained from the absorbance values shown in figure 3. The ratio of absorbances is just the A_{260}/A_{280} . The concentrations were obtained from the absorbances and the fact that a solution of 50 ng/ μ L DS DNA typically has an absorbance of 1.0.

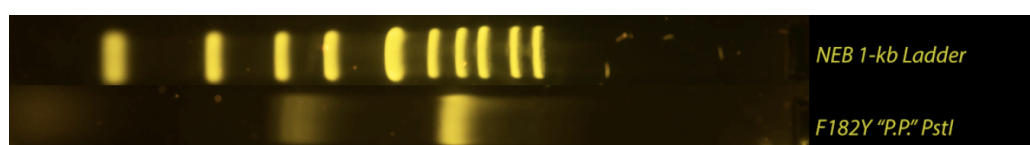


Figure 5: This gel highlights the restriction digest of our purified plasmid with the PstI restriction enzyme.

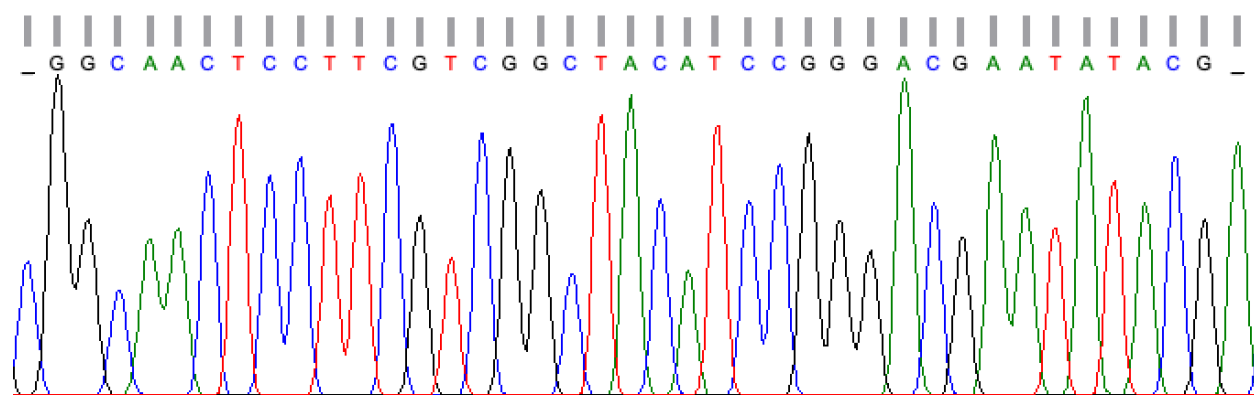


Figure 6: This figure shows one region from our returned capillary electrophoresis sequencing. This region is highlighted because it contains our mutated primers. The bars above the letters represent the confidence in the identity of each base. All of these peaks were well established.

Discussion and Analysis:

Following our site directed mutagenesis, we performed a preliminary gel (Figure 1) on the plasmid products to ensure the plasmids were of relatively appropriate size. These lanes appear to indicate that our plasmids are the appropriate length. The pWhitescript is expected to be approximately 4,500 base pairs long and the pET-14b plasmid is expected to be 5647 base pairs long¹. Although this was just a supplemental assessment, it seems to be fairly accurate and it gave us the confidence in our PCR product to progress further in the procedure at this point.

Our plates highlighted in figure 2 give an idea of the success of our cellular transformation. The ampicillin resistance gene was present in both our pWhitescript control plasmid and our pET-14b mutant urate oxidase plasmid. The β -lactamase gene is the only way which cells on either plate are capable of surviving and reproducing, this means that we know that our transformations succeeded on these cells. The purpose of this plating is two fold. It confirms the success of our transformation and allows us to select a bacterial colony for multiplication. Despite the plates running adequately, the pWhitescript is not as blue as was expected. Part of this is the lighting and picture quality, but still it is challenging to differentiate the white cells from the blue cells. This is most likely due to either a low concentration of X-gal, poor transformation efficiency, or poor functionality of the enzyme. We can assume that the concentration of X-gal is sufficient and we could test the quality of the pWhitescript β -galactosidase gene by performing an additional transformation. The most compelling error is that the transformation of the plasmid into the host XL-1 cells was not particularly successful. This would most likely be the result of a poor heat shock. We may not have placed the cells immediately back on ice or perhaps the cells were in the hot water for too long. Both of these would result in less plasmid DNA uptake.

Figures 3 and 4 highlight the purity of our plasmid sample following the purification by the Plasmid Miniprep Kit. The graph shows significant absorbance at 260 nm, which is expected for the plasmid DNA in the solution and the protein absorbance at 280 nm is significantly lower. The ratio of A_{260}/A_{280} of 1.95 is better than the minimum acceptable value of 1.7. The A_{320} value is near zero and about 3 % of the A_{260} . The concentrations of plasmid in the sample can be calculated as described in figure 4 or using Beer's Law and the approximate molar extinction

coefficient of double stranded DNA. The greatest source of error in this segment of the experiment would derive from small nucleic acid sequences and loose nucleobases in solution. All of these would absorb around 260 nm and inflate our perceived purity of our plasmid.

The second gel electrophoresis highlights the digest of our plasmid with the PstI restriction endonuclease and confirms that our plasmid contains the desired urate oxidase gene. Otherwise, this analysis is not particularly interesting and provides little insight into the success of our mutation. That being said, We expected a cut at position 735 and 4898 such that two fragments of lengths 4163 and 1484 appear in the gel. Both of these bands are present in their expected locations. Although the band corresponding to the 1484 base pair fragment is significantly more blurry, this is not particularly surprising considering the smaller fragments are more susceptible to longitudinal diffusion. This means the smaller fragments have significantly varied distances traveled compared to the larger fragments.

The last and most important figure highlights our results from the sequencing laboratory. Although the entire sequence of urate oxidase was sequenced accurately, the region of the mutation is highlighted because we had already confirmed the presence of the gene in the agarose gel above. The region in figure 6 is identical to the sequence of the primers described in the methods. The bars above the bases represent confidence and all of the bases in the figure were very high because they were relatively central in the plasmid sequence. Residues near the beginning and the end are typically much lower resolution.

Conclusion:

The mutant urate oxidase gene F182Y was successfully implemented into our plasmid. This plasmid was then multiplied, purified and then characterized by electrophoresis capillary sequencing. The implications of this are promising for the next component of this experiment where we will express the protein, purify it, and characterize its activity.

Additional Questions:

- (1) Discuss the Clustal program and how it is used to generate dendrograms and multiple sequence alignments:

Clustal is a computational approach to create phylogenetic trees and multiple sequence alignments. The general procedure can be broken down into a three step algorithm. The first step is the calculation of all pairwise sequence similarities given by $0.5 N (N - 1)^6$. In practice this is a symmetrical matrix, where the $0.5 N$ term accounts for the symmetry and the $N-1$ term accounts for the fact that the diagonal has no useful similarity scores⁶. This is calculated as the number of exactly matching residues between a pair of sequences in the optimal alignment⁶. A penalty is subtracted from the score for gaps⁶. The second step uses the UPGMA algorithm to convert a file of similarity scores and returns a dendrogram as a series of records, one for each cluster⁶. This dendrogram file is used as an input in the multiple alignment program, the third step⁶. Specifically, the original sequences are aligned using the dendrogram file and the Wilbur and Lipman method and the alignment is ready to be displayed⁶.

- (2) Create a MSA for the coronavirus main protease:

This is a multiple sequence alignment of the 13 main protease sequences described. For clarity it has been split in half

NCBI Multiple Sequence Alignment Viewer, Version 1.19.1

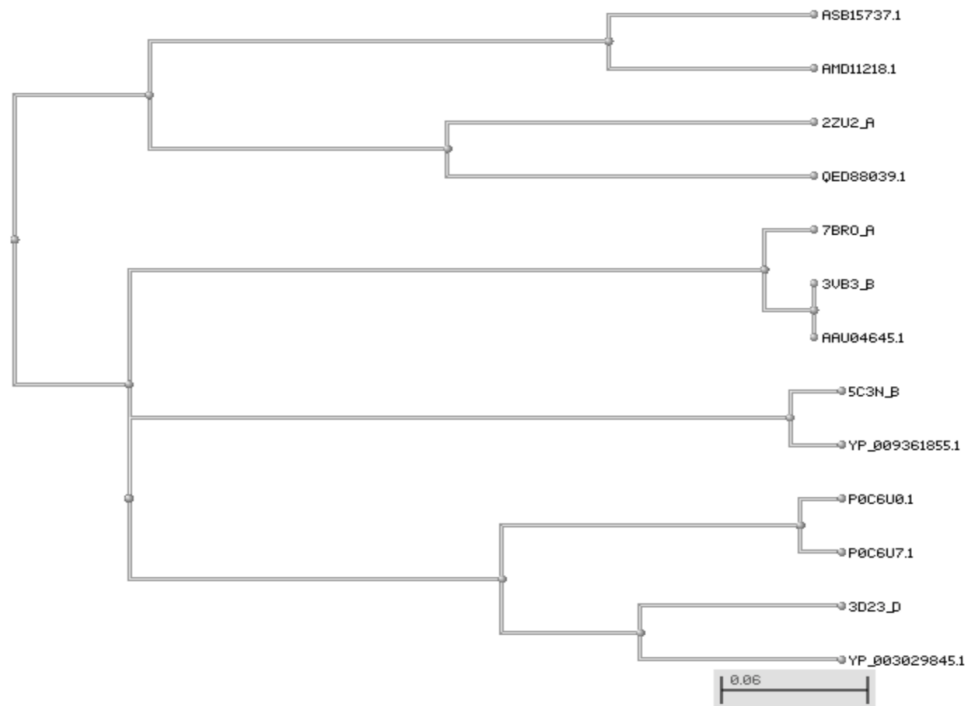
Sequence ID	Alignment	Organism
3D23_D	(+) ELGQKKA PSGKVEKCHVYVGGSTLNGWLDDVPCPRHYICSDHNDHNPYELLCTSTLQVSDG	Human coronavirus H...
7BRQ_A	(+) ELGQKKA PSGKVEKCHVYVGGSTLNGWLDDVPCPRHYICSDHNDHNPYELLCTSTLQVSDG	Severe acute respiratory...
5C3N_B	(+) ELGQKKA PSGKVEKCHVYVGGSTLNGWLDDVPCPRHYICSDHNDHNPYELLCTSTLQVSDG	Middle East respiratory ...
22U2_A	(+) ELGQKKA PSGKVEKCHVYVGGSTLNGWLDDVPCPRHYICSDHNDHNPYELLCTSTLQVSDG	Human coronavirus 229E
3VB3_B	(+) ELGQKKA PSGKVEKCHVYVGGSTLNGWLDDVPCPRHYICSDHNDHNPYELLCTSTLQVSDG	Severe acute respiratory...
PCG6U.1	(+) ELGQKKA PSGKVEKCHVYVGGSTLNGWLDDVPCPRHYICSDHNDHNPYELLCTSTLQVSDG	Bovine coronavirus Mebus
ASB15737.1	(+) ELGQKKA PSGKVEKCHVYVGGSTLNGWLDDVPCPRHYICSDHNDHNPYELLCTSTLQVSDG	Canine coronavirus
AMD17218.1	(+) ELGQKKA PSGKVEKCHVYVGGSTLNGWLDDVPCPRHYICSDHNDHNPYELLCTSTLQVSDG	Feline coronavirus
YP_003029845.1	(+) ELGQKKA PSGKVEKCHVYVGGSTLNGWLDDVPCPRHYICSDHNDHNPYELLCTSTLQVSDG	Rat coronavirus Parker
YP_003029845.1	(+) ELGQKKA PSGKVEKCHVYVGGSTLNGWLDDVPCPRHYICSDHNDHNPYELLCTSTLQVSDG	Rat coronavirus
AAU04645.1	(+) ELGQKKA PSGKVEKCHVYVGGSTLNGWLDDVPCPRHYICSDHNDHNPYELLCTSTLQVSDG	Civet SARS CoV 0072...
PCG6U.1	(+) ELGQKKA PSGKVEKCHVYVGGSTLNGWLDDVPCPRHYICSDHNDHNPYELLCTSTLQVSDG	Human coronavirus OC43
QED88039.1	(+) ELGQKKA PSGKVEKCHVYVGGSTLNGWLDDVPCPRHYICSDHNDHNPYELLCTSTLQVSDG	Human coronavirus NL63

NCBI Multiple Sequence Alignment Viewer, Version 1.19.1

Sequence ID	Alignment	Organism
3D23_D	(+) ELGQKKA PSGKVEKCHVYVGGSTLNGWLDDVPCPRHYICSDHNDHNPYELLCTSTLQVSDG	Human coronavirus H...
7BRQ_A	(+) ELGQKKA PSGKVEKCHVYVGGSTLNGWLDDVPCPRHYICSDHNDHNPYELLCTSTLQVSDG	Severe acute respiratory...
5C3N_B	(+) ELGQKKA PSGKVEKCHVYVGGSTLNGWLDDVPCPRHYICSDHNDHNPYELLCTSTLQVSDG	Middle East respiratory ...
22U2_A	(+) ELGQKKA PSGKVEKCHVYVGGSTLNGWLDDVPCPRHYICSDHNDHNPYELLCTSTLQVSDG	Human coronavirus 229E
3VB3_B	(+) ELGQKKA PSGKVEKCHVYVGGSTLNGWLDDVPCPRHYICSDHNDHNPYELLCTSTLQVSDG	Severe acute respiratory...
PCG6U.1	(+) ELGQKKA PSGKVEKCHVYVGGSTLNGWLDDVPCPRHYICSDHNDHNPYELLCTSTLQVSDG	Bovine coronavirus Mebus
ASB15737.1	(+) ELGQKKA PSGKVEKCHVYVGGSTLNGWLDDVPCPRHYICSDHNDHNPYELLCTSTLQVSDG	Canine coronavirus
AMD17218.1	(+) ELGQKKA PSGKVEKCHVYVGGSTLNGWLDDVPCPRHYICSDHNDHNPYELLCTSTLQVSDG	Feline coronavirus
YP_003029845.1	(+) ELGQKKA PSGKVEKCHVYVGGSTLNGWLDDVPCPRHYICSDHNDHNPYELLCTSTLQVSDG	Rat coronavirus Parker
YP_003029845.1	(+) ELGQKKA PSGKVEKCHVYVGGSTLNGWLDDVPCPRHYICSDHNDHNPYELLCTSTLQVSDG	Rat coronavirus
AAU04645.1	(+) ELGQKKA PSGKVEKCHVYVGGSTLNGWLDDVPCPRHYICSDHNDHNPYELLCTSTLQVSDG	Civet SARS CoV 0072...
PCG6U.1	(+) ELGQKKA PSGKVEKCHVYVGGSTLNGWLDDVPCPRHYICSDHNDHNPYELLCTSTLQVSDG	Human coronavirus OC43
QED88039.1	(+) ELGQKKA PSGKVEKCHVYVGGSTLNGWLDDVPCPRHYICSDHNDHNPYELLCTSTLQVSDG	Human coronavirus NL63

- (3) Describe the evolutionary value of a multiple sequence analysis, how they are used to generate a phylogenetic tree, and create a phylogenetic tree from the previous MSA:

Multiple sequence analysis helps determine evolutionary relationships based on the homology between sequences⁷. In most sequences functional domains are annotated; therefore, a MSA can help determine non annotated sequences⁷. MSA's also find conserved regions of functional importance⁷. The generation of a phylogenetic tree is usually determined by the distances between key functional residues or by pairwise alignment based on similarity scores⁷. The main protease of POC6UO.1 (bovine) is most closely related to that seen in POC6U7.1 (OC43).



References:

- 1) Khan, K; Parsons, S; Kohn, J. Theory Manual: Laboratory Techniques in Biochemistry. Department of Chemistry and Biochemistry University of California, Santa Barbara (2021),
- 2) Oda, M.; Satta, Y.; Takenaka, O.; Takahata, N. Loss of Urate Oxidase Activity in Hominoids and Its Evolutionary Implications. *Molecular Biology and Evolution* **2002**, 19 (5), 640–653.

- 3) Alakel, N.; Middeke, J. M.; Schetelig, J.; Bornhäuser, M. Prevention and Treatment of Tumor Lysis Syndrome, and the Efficacy and Role of Rasburicase. *OncoTargets and Therapy* **2017**, *Volume 10*, 597–605.
- 4) Khan, K. Biochemistry Laboratory Operation Manual (CHEM 125L): The Operations Manual for Component II. Department of Chemistry and Biochemistry University of California, Santa Barbara (2021), 16-20.
- 5) Xie, G.; Yang, W.; Chen, J.; Li, M.; Jiang, N.; Zhao, B.; Chen, S.; Wang, M.; Chen, J. Development of Therapeutic Chimeric Uricase by Exon Replacement/Restoration and Site-Directed Mutagenesis. *International Journal of Molecular Sciences* **2016**, *17* (5), 764.
- 6) Higgins, D. G.; Sharp, P. M. CLUSTAL: A Package for Performing Multiple Sequence Alignment on a Microcomputer. *Gene* **1988**, *73* (1), 237–244.
- 7) Nguyen, K.; Guo, X.; Pan, Y. In *Multiple biological sequence alignment: scoring functions, algorithms and applications*; Wiley Blackwell: Chichester, West Sussex, 2016; pp 103–112.